

# Modelling thermal activation characteristics of the sensitization of thermoluminescence in quartz

Reuven Chen<sup>1</sup> and Vasilis Pagonis<sup>2</sup>

<sup>1</sup> School of Physics and Astronomy, Raymond and Beverly Sackler Faculty of Exact Sciences, Tel-Aviv University, Tel-Aviv 69978, Israel

<sup>2</sup> Physics Department, McDaniel College, Westminster, MD 21158, USA

Received 10 September 2003

Published 19 December 2003

Online at [stacks.iop.org/JPhysD/37/159](http://stacks.iop.org/JPhysD/37/159) (DOI: 10.1088/0022-3727/37/2/003)

## Abstract

The sensitization of the  $\sim 110^\circ\text{C}$  thermoluminescence peak in quartz, also termed the ‘pre-dose’ effect, was previously explained using an energy level model including two electron trapping states and two hole centres. The experimental procedure includes a stage of high temperature activation following a relatively large irradiation of the sample. The response to a small test-dose was found to depend on this activation temperature. With different quartz samples, different behaviours of the thermal activation characteristics (TACs) were found. In typical TACs, the sensitivity reached a maximum at  $\sim 500^\circ\text{C}$ , followed by a rather sharp decline in some samples; in others a maximum was reached at  $\sim 350^\circ\text{C}$  followed by a slight decline towards a plateau level. In this work, we show that these behaviours can rather easily be explained within the framework of the two traps–two centres model. This is done by numerical solution of the relevant sets of differential equations governing the different stages of the experimental procedure. The different kinds of dependence were simulated with different sets of trapping parameters. A better insight into the processes taking place is reached, which may have implications in the application of pre-dose dating of archaeological quartz samples and in retrospective dosimetry.

## 1. Introduction

The sensitization of various thermoluminescence (TL) materials by  $\beta$  or  $\gamma$  irradiations followed by activation at high temperature is a quite well-known phenomenon (see, e.g. Cameron *et al* [1], Zimmerman [2, 3], Aitken [4], Chen [5], Yang and McKeever [6], Bailiff [7] and Pagonis *et al* [8]). By sensitization one means the change of sensitivity, namely the response to a given (usually small) test-dose, by a heavier irradiation, followed by a thermal activation. In particular, this effect was reported by Fleming and Thompson [9] and by others in quartz, and therefore it is of importance when dealing with the dating of archaeological pottery [10] and with retrospective dosimetry [7]. The sensitization effect, also called the pre-dose effect, of the  $110^\circ\text{C}$  peak in quartz has further been reported by Zimmerman [2] who also gave a model to account for the phenomenon. Briefly, the Zimmerman

model deals with an electron trapping state T and two hole centres, R and L. The cross section for trapping holes is assumed to be much larger for R than for L, and therefore, during irradiation, practically all the free holes accumulate in R whereas the generated electrons (or at least some of them—see later) concentrate in T. This trap is, however, rather shallow (yielding a peak at  $\sim 110^\circ\text{C}$  at a heating rate of  $5^\circ\text{C s}^{-1}$ ), and is emptied at room temperature within hours, or may be emptied by heating to, say,  $150^\circ\text{C}$ . It is assumed that R is not a very deep state in the sense that it is close enough to the valence band so that heating, say, to  $\sim 500^\circ\text{C}$  would release the holes from R. Although the probability of their trapping in L is rather low, as mentioned above, at this high temperature the favourable direction of the holes is to go from R to L. This is so since L is assumed to be much further from the valence band so that once a hole is captured at L, it cannot be thermally released back to the valence band. In this sense, R is a ‘reservoir’

which holds holes following the irradiation and prior to the thermal activation. The increase of the concentration of holes in L represents, according to Zimmerman [2] an increase in the sensitivity, since L is the luminescence centre, the transition into which yields the measured 110°C peak.

Chen [5] suggested an amendment to the Zimmerman model. He argued that since the measured response of the TL to a test-dose is a monotonically increasing function of the concentration of trapped holes in L following the ‘large’ excitation plus thermal activation, on one hand, and also a monotonically increasing function (sometimes linear) of the size of the test-dose on the other hand, the existence of a second trapping state for electrons is to be assumed. This has to be a deeper trap, and should act as a competitor to the released electrons during the ‘read-out’ stage in which the sample is heated following the application of the test-dose, and the emission is recorded at ~110°C. Let us denote from here on the shallower trap by T and the competitor by S (see figure 1). For more details see Chen [5] and Chen and McKeever [11].

The activation temperature was quoted above as 500°C. According to Aitken [12], depending on the type of quartz and the temperature and duration of firing of archaeological quartz in antiquity, there are significant variations of the thermal activation characteristic (TAC) by heating the sample to successively increasing temperatures from 200°C upwards, the sensitivity being measured after each heating. Aitken [12] (figure 3.9) describes in detail a graph previously presented by Fleming and Thompson [9]. This is redrawn in figure 2 here; curve (b) shows ‘early activation’ at ~350°C and curve (a) a ‘late activation’ at ~520°C. Aitken assumes a distribution of hole traps and suggests that the form of the TAC reflects this distribution in a manner that traps close to the valence band have their holes transferred to the L centres at a lower temperature than traps that are not as close. An important feature seen in figure 2 is that the sensitivity reaches a maximum and falls off when higher temperatures are used. This is referred to as thermal deactivation which, according to Aitken [12] is presumed to be due to thermal eviction of holes

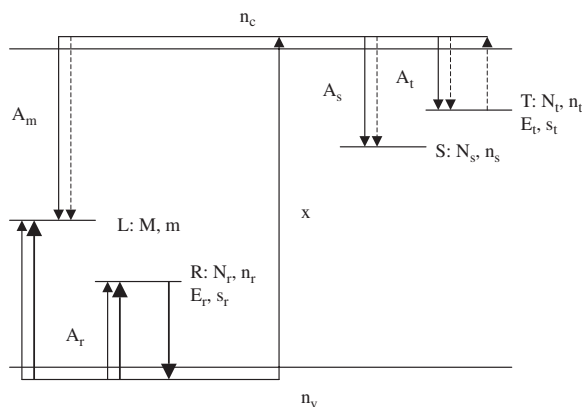


**Figure 1.** An energy-level diagram including the electron trapping state, T, the competitor, S, the hole reservoir, R and the luminescence centre L.  $n_c$  and  $n_v$  are the free electron and hole concentrations, respectively, and  $x$  is the rate of production of free electrons and holes. The thin solid arrows indicate transitions during excitation, the bold solid arrows are transitions taking place during the high temperature activation and the dotted arrows show transitions occurring during the heating to ~150°C.

from L centres into the valence band. Aitken points out that the temperature at which the sensitivity maximum of the TAC is reached depends on the time spent at high temperature. If the heating rate is slow, and more particularly, if the maximum temperature is held for, say, a minute before cut off, then the maximum will shift downwards in temperature. Obviously, when different samples are compared, it is essential that exactly the same thermal treatment is maintained in all activations.

Other works on the pre-dose sensitization include a paper by David and Sunta [13] who reported on their experimental results, which showed that the optimum temperature of activation is dependent on growth conditions of the quartz crystal, and therefore correlated with the formation temperature of the natural quartz. Haskell and Bailiff [14] discuss the retrospective dosimetry of bricks using the sensitivity changes in quartz. They describe the details of the TACs which, generally speaking, show a significant increase in sensitivity starting with activation at ~250°C, reaching a maximum at 500–550°C and decreasing to rather low values (<10% of the maximum) following activation at ~700°C. Chen *et al* [15] compared the TACs for the 110°C TL peak and for the related phenomenon of OSL in quartz, and found rather similar results.

Two independent groups have recently simulated the pre-dose effect of the ~110°C peak in quartz. Figel and Goedicke [16] gave a model with two electron trapping states and three hole centres, the reservoir R and the centres  $L_1$  and  $L_2$ , associated with the two kinds of TL emission in quartz at 380 and at 460 nm. Apart from the addition of a second centre, the model is very similar to that by Chen [5], with one significant difference, namely, that Figel and Goedicke considered the competitor denoted above by S to be thermally connected. They assumed that the electrons in S may be thermally evicted into the conduction band, which may bring about the reduction of sensitivity at temperatures above ~550°C due to the recombination of the released electrons with trapped holes. Chen and Leung [17, 18], using the original model by Chen [5] of two trapping states, T thermally connected and S thermally disconnected, as well as the reservoir R and the luminescence centre L, elaborated upon the dependence of the sensitivity on several dose increments and showed that, as previously

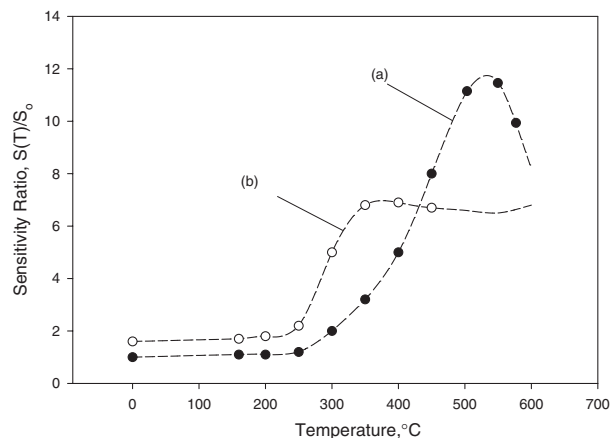


**Figure 2.** The data of Fleming and Thompson [9] redrawn. Curves (a) and (b) show the ‘late activation’ and ‘early activation’ phenomena, respectively.

found experimentally, the behaviour could be presented as an exponential dependence on the accumulated dose  $D$ . Chen and Leung did not explain the TAC behaviour within the framework of their model.

The main purpose of this work is to offer an explanation different from that given by Figel and Goedicke to the TAC of the 110°C peak in quartz. It is demonstrated by numerical simulation and also explained on an intuitive basis that the different kinds of measured TACs can be reached by using the two trap–two centre model and one need not resort to assuming a whole distribution of R centres, as suggested by Aitken, or to the thermal release of competitor traps, as suggested by Figel and Goedicke [16]. Furthermore, the deactivation occurring at higher temperatures is shown to be a direct result of this simpler model, rather than assuming that deactivation is due to thermal eviction of holes from L [12].

## 2. The model

The description of the energy level model given by Chen and Leung [17] is briefly repeated, and shown in figure 1. The transitions shown are during the excitation and during the read-out stages (see figure caption). T is the active trapping state having a concentration of  $N_t$  ( $\text{cm}^{-3}$ ) and an instantaneous occupancy  $n_t$  ( $\text{cm}^{-3}$ ); the activation energy is  $E_t$  (eV) and the frequency factor  $s_t$  ( $\text{s}^{-1}$ ). S is the thermally disconnected trapping state with concentration  $N_s$  ( $\text{cm}^{-3}$ ) and occupancy of  $n_s$  ( $\text{cm}^{-3}$ ).  $A_t$  ( $\text{cm}^3 \text{s}^{-1}$ ) and  $A_s$  ( $\text{cm}^3 \text{s}^{-1}$ ) are the trapping coefficients into T and S, respectively. L is the luminescence centre with concentration  $M$  ( $\text{cm}^{-3}$ ) and instantaneous occupancy of  $m$  ( $\text{cm}^{-3}$ ). The transition coefficient of the free holes from the valence band into L is  $A_l$  ( $\text{cm}^3 \text{s}^{-1}$ ) and the recombination coefficient of free holes is  $A_m$  ( $\text{cm}^3 \text{s}^{-1}$ ). R is the reservoir having a concentration of  $N_r$  ( $\text{cm}^{-3}$ ) and instantaneous occupancy of  $n_r$  ( $\text{cm}^{-3}$ );  $E_r$  (eV) is the activation energy of freeing holes into the valence band and  $s_r$  ( $\text{s}^{-1}$ ) the relevant frequency factor. The rate at which electron–hole pairs are produced by the irradiation is  $x$  ( $\text{cm}^{-3} \text{s}^{-1}$ ), which is proportional to the dose-rate imparted on the sample. Thus, if the irradiation time is  $t_D$ , the total dose given to the sample is proportional to  $x \cdot t_D$  ( $\text{cm}^{-3}$ ), which, in fact, is the concentration of electrons and holes produced by the irradiation per unit volume.

The set of equations governing the process during the excitation stage and that governing the process during the heating stage were given by Chen and Leung [17] and will not be repeated here. The set of equations (2)–(7) in [17] has been solved for certain sets of the parameters using the ode23s Matlab package solver. This particular solver is designed to deal with ‘stiff’ sets of equations and the present set is such a one, in particular, since in equations (4), (5) and (7) in [17], the derivative on the left-hand side is given as a small difference between two large quantities. In parallel, the same equations were solved using the Mathematica differential equations solver, and the results found were practically the same. Of course, the procedure described here which takes care of the process of excitation, is being used for both the test-dose and high-dose simulations.

A second part of the procedure deals with the transitions taking place during the heating of the sample, also shown in

figure 1. In order to simulate more accurately the experimental procedure, we have to add an intermediate stage of ‘relaxation’ in which the irradiation has ceased, and the set of equations is solved with  $x = 0$  for a period of time so as to bring  $n_c$  and  $n_v$  down to negligible values. We then take the final values of  $n_t$ ,  $n_s$ ,  $m$  and  $n_r$  at the end of the relaxation time as initial values for the heating stage.

We assume now that during the high temperature heating, thermal release of holes is possible from the reservoir R (this is at the basis of the Zimmerman model), which may be trapped preferably in L, and that holes from L cannot be thermally released into the valence band in the relevant temperature range. The rate equations governing the process here are equations (8)–(13) in [17]. This second set of equations was also solved using both the ode23s Matlab solver and the Mathematica solver, and the results were found to be the same.

The intensity of the emitted light is assumed to be the result of recombination of free electrons with trapped holes in the centres. Therefore, it is given by

$$I(T) = A_m m n_c. \quad (1)$$

In the simulation, the conventional linear heating function,  $T(t) = T_0 + \beta t$ , is used, where  $\beta$  is the constant heating rate, chosen to be  $5^\circ \text{C s}^{-1}$ .

Two important points are to be mentioned with regard to the simulations reported here. One is that we always start the simulations with empty traps and centres. This is usually considered to be the case in samples previously annealed at high enough temperature. The other point is that we have simulated here the ‘multi-aliquot’ case, namely, that for the measurement of  $S(T)$ , the sample is heated to a temperature  $T$ , and when the sensitivity is to be measured at another value of  $T$ , a different aliquot of the same weight is given the same irradiation, activated at the new temperature and then given the test-dose to find the value of  $S(T)$  as a function of the temperature.

## 3. Numerical results

The parameters were chosen so as to demonstrate the possibility of getting numerical results which mimic those given by Fleming and Thompson [9] and Aitken [12]. The graph by Fleming and Thompson is reproduced in figure 2. The parameters were rather similar to those chosen by Chen and Leung [17, 18], with some changes. Figure 3 resembles the TAC curve (b) in figure 2 which reaches a maximum at  $\sim 350^\circ \text{C}$ , followed by a slight decrease, and then by a plateau for activation temperatures above  $400^\circ \text{C}$ . The main difference as compared to the Chen–Leung parameters is the inversion of the values of  $A_s$  and  $A_m$ , and a small change in the value of  $E_r$ . The values used were:  $s_t = 10^{13} \text{s}^{-1}$ ;  $E_t = 1.0 \text{eV}$ ;  $s_r = 10^{13} \text{s}^{-1}$ ;  $E_r = 1.6 \text{eV}$ ;  $A_t = 10^{-12} \text{cm}^3 \text{s}^{-1}$ ;  $A_r = 10^{-10} \text{cm}^3 \text{s}^{-1}$ ;  $A_s = 10^{-12} \text{cm}^3 \text{s}^{-1}$ ;  $A_m = 10^{-11} \text{cm}^3 \text{s}^{-1}$ ;  $A_l = 10^{-12} \text{cm}^3 \text{s}^{-1}$ ;  $N_t = 10^{13} \text{cm}^{-3}$ ;  $N_s = 10^{13} \text{cm}^{-3}$ ;  $N_r = 10^{13} \text{cm}^{-3}$ ;  $M = 10^{14} \text{cm}^{-3}$ ;  $x = 10^9 \text{cm}^{-3} \text{s}^{-1}$  and  $t_D = 3000 \text{s}$  for the ‘long’ excitation and  $t = 1 \text{s}$  for the test-dose.

Figure 4(c) simulates the sensitivity shown in curve (a) in figure 2. Curves (a) and (b) give the dependences of

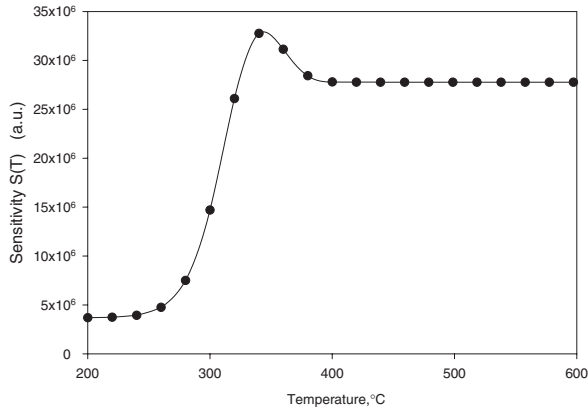


**Figure 3.** A simulated TAC, in which the curve reaches a maximum at  $\sim 350^\circ\text{C}$ , decreases slightly and reaches a plateau at higher temperatures. The parameters used are given in the text.

$n_t$  (following a given test-dose irradiation) and of  $m$  on the activation temperature, which helps the explanation of curve (c) as elaborated below. The parameters here are the same as in figure 3, except that  $E_r$  was changed to 1.8 eV;  $s_r$  to  $10^{10} \text{ s}^{-1}$  and  $t_D$  to 7000 s. The results are a good simulation of curve (a) by Aitken in the sense that the sensitivity increases with the activation temperature, reaching a maximum at  $\sim 520^\circ\text{C}$  and reducing significantly at  $\sim 650^\circ\text{C}$ . The behaviour at higher temperatures is not seen in the experimental graph.

Figure 5 shows the results of the simulation of the test-dose dependence of the measured  $\sim 110^\circ\text{C}$  TL peak (curve (a)) and of the natural-simulated ‘large’ dose (curve (b)), as a function of the activation temperature. In curve (a), the maximum intensity both at the optimal activation temperature and lower and higher temperatures is seen to be practically linear with the test-dose. In curve (b), it is seen that the whole TAC curve goes up with increase in the natural-simulated dose, monotonically though sub-linearly, when the size of the test-dose is kept constant. The sublinearity appears to be a result of the filling of the recombination centre M.

#### 4. Discussion

The main achievement of this work is that it is possible to explain the peak-shaped TAC appearing in several quartz samples, using the two trap–two centre model. This behaviour has been found numerically as shown in figure 4(c); we would like to give an intuitive explanation for this result. The processes involved are quite complex and the explanation is rather subtle. In order to understand the peak shape shown in figure 4(c), we should consider the curves of  $n_t$  and  $m$  as a function of the activation temperature following a given excitation dose as shown in figures 4(a) and (b).  $m(T)$  shown in figure 4(b) is the concentration of holes in the recombination centre following the ‘large’ excitation which brings a large number of holes into  $n_r$  and a small number of holes directly into  $m$ . The heating to a temperature  $T$  within the given range transfers holes from  $N_r$  into  $M$ , so that when the sample is cooled back to room temperature, the value of  $m$  is determined to be an increasing function of the activation temperature  $T$  as seen in curve (b).

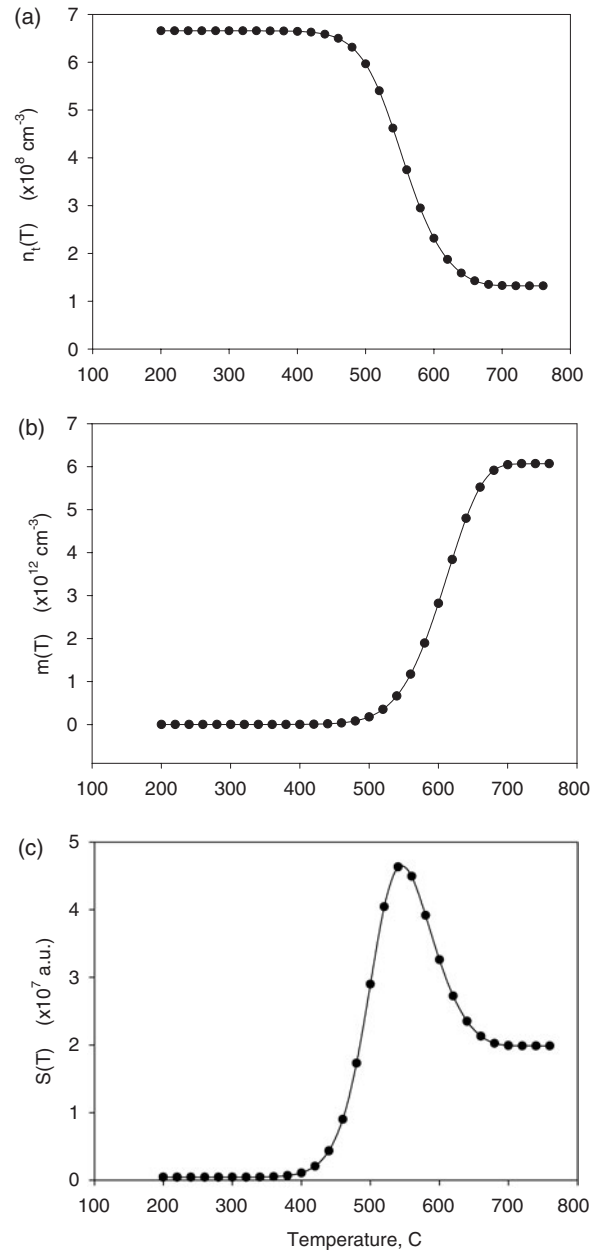


**Figure 4.** For a chosen set of parameters,  $n_t$  at the end of the test-dose excitation as a function of the activation temperature  $T$  is shown on (a); the occupancy of the recombination centres as a function of  $T$  is shown in (b) and the resulting sensitivity  $S(T)$  is given in (c). The parameters are given in the text.

As for  $n_t(T)$  shown in curve (a), it should be noted that these are the values calculated following the administration of the test-dose subsequent to the application of the ‘high’ dose and activation at temperature  $T$ . This point is illustrated by the fact that in the example shown, the values of  $n_t$  are in the range  $1 \times 10^8 - 7 \times 10^8 \text{ cm}^{-3}$  as compared to the values of  $m$  which go up to  $7 \times 10^{12} \text{ cm}^{-3}$ . The dependence of this  $n_t(T)$  is a result of the dependence of  $m$  on the activation temperature. When the test-dose is imparted, the larger the value of  $m$ , the more the number of electrons that are ‘lost’ through the recombination, which takes place during this ‘short’ irradiation, and therefore at the end of the irradiation less electrons are trapped at the

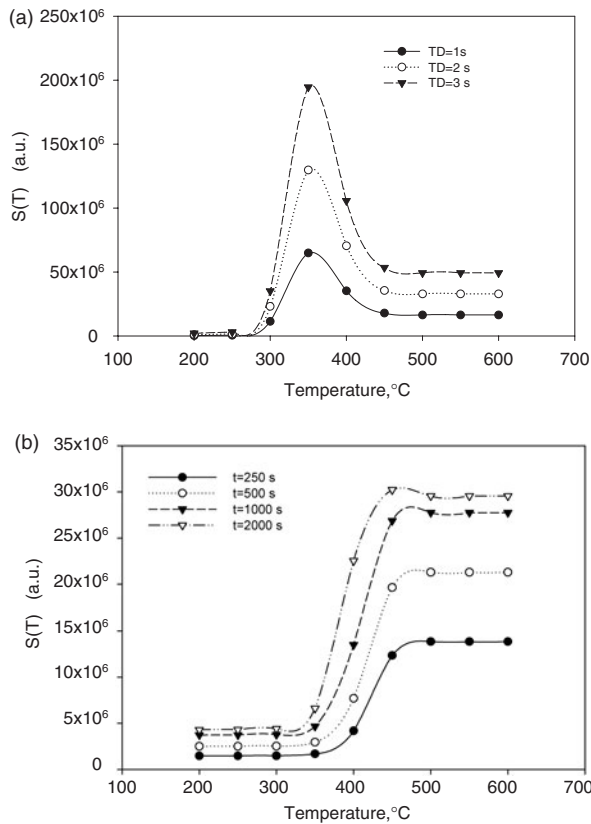


**Figure 5.** The dependence of the simulated intensity as a function of the activation temperature is shown in (a) for three test-doses with relative values of 1 : 2 : 3. In (b), the curves shown are of the TACs for simulated-natural doses with relative values of 1 : 2 : 3 : 4. The set of parameters used is the same as that in figure 3.

active trapping state  $N_t$ . This explains the decreasing function  $n_t(T)$ . During the following ‘short’ heating, to  $\sim 150^\circ\text{C}$ , fewer electrons reach the conduction band, and therefore, for higher activation temperatures, the concentration of free electrons  $n_c$  will be smaller. It should be stressed that, of course, the values of  $n_c$  are associated with the temperature of heating following the test-dose irradiation; however, here, we are interested in their dependence on the temperature of activation  $T$ . It should also be noted that since the test-dose is relatively small,  $m$  changes only slightly due to recombination during the test-dose irradiation. For a qualitative description, let us assume that  $n_c$  as a function of  $T$  behaves, more or less, like  $n_t(T)$ . Finally, the TL intensity following the test-dose excitation is given by equation (1), namely, it is proportional to  $m$  and  $n_c$ . As long as  $n_c$  behaves as a function of the activation temperature like  $n_t(T)$ ,  $S(T)$  should look like the product of the two curves, the decreasing function in (a) and the increasing one in (b) of figure 4. The product function yields a peak-shaped curve like the one shown in figure 4(c). It should be noted that whereas this explanation (in particular regarding the relation between  $n_t$  and  $n_c$ ) is intuitive but not rigorous, the results shown in figures 4(a)–(c) are those of the numerical solution of the relevant sets of differential equations in the appropriate sequence, and therefore are even more convincing in demonstrating the possibility of explaining the peak-shaped curve of the TAC. Another point to be mentioned is that in figure 4(c),  $S(T)$  goes to under 50% of the maximum value.

In some experimental cases, the reduction was even more dramatic. With the present model, with another choice of the set of parameters, such a decrease can easily be reached, but figure 4(c) is sufficient to demonstrate the effect.

As pointed out above, figure 5 demonstrates the capability of the model to explain the experimental results of the approximately linear dependence of the TL intensity on the size of the test-dose, and the monotonic dependence of the emitted TL on the size of the natural-simulated dose.

It is noted that the results of the simulation may have important practical implications for the application of pre-dose dating in quartz samples and in retrospective dosimetry. The results of figure 5(b) shows that aliquots of the same quartz sample can exhibit significant variations in the location of the maximum TL sensitivity, which corresponds to the optimum activation temperature used during application of the pre-dose technique. Specifically, figure 5(b) suggests that these variations in the activation temperature may be due to the aliquots having received different doses in nature.

Furthermore, the results of figure 4 show that the exact shape of the TAC and the location of the optimum activation temperature are the results of the complex competition process between the two concentrations  $n_t(T)$  and  $m(T)$  shown in figures 4(a) and (b).

## 5. Conclusion

In this work, we have demonstrated that the usually seen behaviour of the TAC can be directly explained in the framework of a relatively simple model. The model includes one recombination centre, one reservoir, one active trap, and one disconnected trap, which competes with the active trap and the recombination centre for free electrons both during the excitation and the heating of the quartz sample. In fact, this is the model originally given by Zimmerman [2] and later amended by Chen [5]. What is new here is that the special behaviour of the TACs in some quartz samples, namely, that it reaches a maximum at  $\sim 520^\circ\text{C}$  and decreases substantially at higher activation temperatures, is directly shown to result from the model without the need to assume either the possibility that holes are thermally evicted to the valence band as suggested by Aitken [12], or that the competing trapping state can thermally release electrons as suggested by Figel and Goedicke [16]. Concerning the Aitken assertion, it should be mentioned that the possibility of releasing thermally holes from the centres to the valence band is not very reasonable, since the band gap of quartz is  $\sim 8.5$  eV [19] and the emission photons resulting from transition from the conduction band into the centre are  $\sim 3.3$  eV (corresponding to the wavelength of 380 nm). This puts the hole centres  $>5$  eV above the valence band, and they cannot be thermally released at the temperature range in question.

In view of the results reported here, it is hard to tell whether the peak shape of the TAC reported by Figel and Goedicke results indeed from the thermal release of electrons from the competitor as suggested by them, or would be observed anyway, without the thermal release from the deep traps, as demonstrated here. The features described are explained both using intuitive considerations and by numerical simulation which follows the experimental steps taken in the process of measuring the TAC. It should be mentioned that we do

not claim to have the exact set of parameters related to the mentioned experimental curve (curve (a) in figure 2), but rather that we can easily choose a set of parameters that yields the general shape of  $S(T)$ . In fact, while comparing this experimental curve to our figure 4(c), it can be seen that when the experimental curve starts to increase at  $\sim 300^\circ\text{C}$ , the theoretical one takes off at  $\sim 400^\circ\text{C}$  although both of them reach a maximum at  $\sim 520^\circ\text{C}$ . The simple explanation is that whereas the simulation attempts to show the essence of the behaviour within the framework of the simplest possible model, in the real material there probably are perturbations such as additional trapping states and centres that may change the details of the measured phenomena. The behaviour seen in other samples, in which the TAC reaches a maximum at a certain temperature (e.g.  $\sim 350^\circ\text{C}$ ), reduces slightly and remains constant for higher activation temperatures, is also demonstrated and shown to result directly from the model, using different sets of parameters. All the sets of parameters used are within the same range as those reported in the literature [16, 20]. It should be noted that there is no uniquely accepted set of parameters in the literature, which simply reflects the fact that there are significant variations in the parameters between different samples, which among other things is exhibited in the large variations in brightness of different samples. Finally, the nearly linear dose-rate dependence of TL as well as the monotonically increasing dependence on the natural dose are also explained within this rather simple model.

## References

- [1] Cameron J R, Suntharalingam N and Kenney G N 1968 *Thermoluminescence Dosimetry* (Madison: The University of Wisconsin Press)
- [2] Zimmerman J 1971 *J. Phys. C: Solid State Phys.* **4** 3265–76
- [3] Zimmerman J 1971 *J. Phys. C: Solid State Phys.* **4** 3277–91
- [4] Aitken M J 1974 *Physics and Archaeology* (Oxford: Clarendon) p 124
- [5] Chen R 1979 *Eur. PACT J.* **3** 325–35
- [6] Yang X and McKeever S W S 1990 *J. Phys. D: Appl. Phys.* **23** 237–44
- [7] Bailiff I K 1994 *Radiat. Meas.* **23** 471–9
- [8] Pagonis V, Kitis G and Chen R 2003 *Radiat. Meas.* **37** 267–74
- [9] Fleming S J and Thompson J 1970 *Health Phys.* **18** 567–8
- [10] Fleming S J 1973 *Archaeometry* **15** 13–30
- [11] Chen R and McKeever S W S *Theory of Thermoluminescence and Related Phenomena* (Singapore: World Scientific) p 208
- [12] Aitken M J 1985 *Thermoluminescence Dating* (London: Academic) p 158
- [13] David M and Sunta C M 1983 *Indian J. Pure Appl. Phys.* **21** 659–60
- [14] Haskell E H and Bailiff I K 1990 *Radiat. Prot. Dosim.* **34** 195–7
- [15] Chen G, Li S H and Murray A S 2000 *Radiat. Meas.* **32** 641–5
- [16] Figel M and Goedicke C 1999 *Radiat. Prot. Dosim.* **84** 433–8
- [17] Chen R and Leung P L 1998 *J. Phys. D: Appl. Phys.* **31** 2628–35
- [18] Chen R and Leung P L 1999 *Radiat. Prot. Dosim.* **84** 43–6
- [19] Fleming S J 1979 *Thermoluminescence Techniques in Archaeology* (Oxford: Clarendon) p 84
- [20] Bailey R M 2001 *Radiat. Meas.* **33** 17–45